INSTITUTE OF PHYSICS PUBLISHING PLASMA SOURCES SCIENCE AND TECHNOLOGY

Plasma Sources Sci. Technol. **14** (2005) 751–756 doi:10.1088/0963-0252/14/4/014

Theoretical study of pulsed microwave discharge in nitrogen

Z Bonaventura, D Trunec, M Meško, P Vašina and V Kudrle

Department of Physical Electronics, Faculty of Science, Masaryk University, Kotlářská 2, 611 37 Brno, Czech Republic

E-mail: zbona@physics.muni.cz

Received 7 March 2005
Published 18 October 2005
Online at stacks.iop.org/PSST/14/751

Abstract

A pulsed microwave discharge burning in pure nitrogen was studied theoretically. The time-dependent Boltzmann equation for electrons was solved numerically in multi-term approximation. It was assumed that the discharge was ignited by a 100 kW microwave ($f = 9.4$ GHz) pulses with 2.5 μs duration; the repetition frequency was 400 Hz. It was shown that the electron distribution function approaches very quickly the steady state distribution function after a change of the amplitude of electric field intensity. The steady state time averaged values of electron mean energy, diffusion and rate coefficients and drift velocity were calculated for different values of electric field intensity. With these values the actual values of electric field intensity from a previous experiment were determined from the measured time dependence of electron concentration. The calculated values were compared with previous experimental results.

1. Introduction

Microwave excited discharges are often used because of the lack of electrodes and the comparatively high density of charge carriers and radicals. Pulsed discharges have additional parameters, i.e. pulse duration and repetition frequency, which enable us to control the parameters of produced plasma. Recently the pulsed microwave discharges in nitrogen were studied experimentally by Baeva *et al* [1] and Meško *et al* [2]. Baeva *et al* [3] also presented a theoretical study concerning their experimental results. They solved the Boltzmann equation for electrons in the effective field approximation (EFA) coupled with the master equations for vibrational levels of nitrogen. Furthermore, they used a two-term approximation in the expansion of the distribution function in Legendre polynomials. Other references on modelling of discharges in nitrogen can be found in [3].

The main aim of this paper is to complete and interpret the experimental data in our previous work concerning pulsed microwave discharges in nitrogen [2]. The plasma in this experiment was produced in a spherical glass vessel with the inner diameter, R, of 50 cm. From one side the vessel was irradiated by a horn antenna, and microwaves were focused by the dielectric lens in the centre of the vessel. An aluminium foil was placed on the opposite side wall in order to reflect and focus the microwaves. Microwaves (x-band) were generated by pulse magnetron (peak power reaches 100 kW). The pulses had a 2.5 μs duration and a repetition frequency 400 Hz. The pulses had a rectangular shape with the rising and falling time of the edges of 10 ns. The time dependence of electron concentration was measured by a microwave method, which was already successfully used for electron concentration measurement in afterglow plasmas [4]. The time resolved optical emission spectroscopy and transmitted power measurement were also performed. The electron kinetics in the discharge was described by the Boltzmann equation for spatially homogeneous plasma. Because the microwave power was supplied to the discharge in short pulses, we considered first the fully time-dependent Boltzmann equation. A new simple numerical technique to solve the time-dependent Boltzmann equation was used. However, it was found that the distribution function relaxes very quickly to the steady state distribution function after a change and that the changes of macroscopic parameters during one period of the microwave power are small under our conditions. This allowed us to use time averaged values of collision frequencies, mean energy, etc for further calculations of electric field intensity. The results of the calculation were compared with the experimental data.

2. Boltzmann equation

The time-dependent distribution function of electrons in the discharge was calculated using the spatially homogenous Boltzmann equation:

$$\frac{\partial}{\partial t}F - \frac{e_0}{m_\mathrm{e}}\boldsymbol{E}\cdot\frac{\partial}{\partial \boldsymbol{v}}F = C^\mathrm{el} + \sum_m C_m^\mathrm{in}, \tag{1}$$

where $F(\boldsymbol{v}, t)$ is the distribution function of electrons and m_e and $-e_0$ are the mass and the charge of electron. C^el and C_m^in are elastic and inelastic collision integrals for the collisions of electrons with neutral gas particles (mass M and density N). The gas particles are assumed to be at rest. For simplicity the elastic and all inelastic collisions were assumed to be isotropic. The electric field $\boldsymbol{E}$ was chosen to be parallel to the z-axis, i.e. $\boldsymbol{E} = E_0 \sin\omega t \boldsymbol{e}_z$. In this case the distribution function has reduced velocity dependence $F(\boldsymbol{v}, t) = F(v, v_z/v, t)$, and it can be expanded in Legendre polynomials $P_n(v_z/v)$ and approximated by an arbitrary number l of terms:

$$F(v, v_z/v, t) = \sum_{n=0}^{l-1} F_n(v, t) P_n(v_z/v). \tag{2}$$

Substituting this expansion to the Boltzmann equation we obtain the hierarchy of partial differential equations:

$$\begin{aligned}
&\frac{\partial}{\partial t}f_0 - \frac{e_0}{3}\left(\frac{2}{m_\mathrm{e}U}\right)^{1/2} E(t)\frac{\partial}{\partial U}(Uf_1) \\
&\quad - U^{-1/2}\frac{\partial}{\partial U}\left(U^{3/2}\frac{2m_\mathrm{e}}{M}\nu^\mathrm{el}(U) f_0\right) + \sum_m \nu_m^\mathrm{in}(U) f_0 \\
&\quad - \sum_m \left(\frac{U+U_m^\mathrm{in}}{U}\right)^{1/2} \nu_m^\mathrm{in}(U+U_m^\mathrm{in})\, f_0(U+U_m^\mathrm{in}) = 0,
\end{aligned} \tag{3}$$

$$\begin{aligned}
&\frac{\partial}{\partial t}f_n - \frac{n}{2n-1}\left(\frac{2}{m_\mathrm{e}}\right)^{1/2} e_0 E(t) \\
&\quad \times\left[U^{1/2}\frac{\partial}{\partial U}f_{n-1} - \frac{n-1}{2}U^{-1/2} f_{n-1}\right] \\
&\quad - \frac{n+1}{2n+3}\left(\frac{2}{m_\mathrm{e}}\right)^{1/2} e_0 E(t) \\
&\quad \times\left[U^{1/2}\frac{\partial}{\partial U}f_{n+1} + \frac{n+2}{2}U^{-1/2} f_{n+1}\right] \\
&\quad + \left(\nu^\mathrm{el}(U) + \sum_m \nu_m^\mathrm{in}(U)\right) f_n = 0, \qquad 1 \leqslant n \leqslant l-2
\end{aligned} \tag{4}$$

$$\begin{aligned}
&\frac{\partial}{\partial t}f_{l-1} - \frac{l-1}{2l-3}\left(\frac{2}{m_\mathrm{e}}\right)^{1/2} e_0 E(t) \\
&\quad \times\left[U^{1/2}\frac{\partial}{\partial U}f_{l-2} - \frac{l-2}{2}U^{-1/2} f_{l-2}\right] \\
&\quad + \left(\nu^\mathrm{el}(U) + \sum_m \nu_m^\mathrm{in}(U)\right) f_{l-1} = 0,
\end{aligned} \tag{5}$$

for the expansion coefficients

$$f_n(U, t) = 2\pi\left(\frac{2}{m_\mathrm{e}}\right)^{3/2} F_n(v(U), t). \tag{6}$$

Here $U = m_\mathrm{e}v^2/2$ is the electron energy and U_m^in is the energy loss in the mth inelastic process. In deriving this hierarchy a further expansion of each collision integral with respect to the ratio m_e/M of the electron-to-gas particle masses has been performed; only a leading term has been taken into account. The quantities,

$$\nu^\mathrm{el}(U) = \left(\frac{2}{m_\mathrm{e}}\right)^{1/2} U^{1/2} N Q^\mathrm{m}(U), \tag{7}$$

$$\nu_m^\mathrm{in}(U) = \left(\frac{2}{m_\mathrm{e}}\right)^{1/2} U^{1/2} N Q_m^\mathrm{in}(U), \tag{8}$$

are the collision frequencies for elastic and inelastic collisions, where Q^m and Q_m^in denote the cross sections for momentum transfer and mth inelastic collision. The cross section for electron–nitrogen collision were taken from [5].

Usually only the first two terms are taken into account in expansion (2). This approach to nitrogen can lead to inaccurate results because there are large inelastic cross sections at low electron energies [6]. Also the time-dependent problems need to consider more terms in order to obtain a correct solution [7]. In our calculation 150 terms in expansion (2) were taken. Review papers on theoretical studies of electron behaviour in different electric and magnetic fields can be found in [8–10].

3. Numerical procedure

The system of equations (3)–(5) given above was solved as an initial-boundary value problem. The boundary conditions are given by relations:

$$\begin{aligned}
&f_0(U \geqslant U_\infty, t) = 0, \\
&f_n(U = 0, t) = 0 \qquad n \geqslant 1, \\
&f_n(U \geqslant U_\infty, t) = 0 \qquad n \geqslant 1,
\end{aligned} \tag{9}$$

where U_∞ is sufficiently large energy, together with the condition

$$\left.\frac{\partial f_0}{\partial U}\right|_{U=0} = 0.$$

A detailed derivation of these boundary conditions can be found in [11]. A new numerical method for the solution of time-dependent Boltzmann equation was used as follows. The system of equations (3)–(5) was discretized in energy space on a uniform mesh U_i:

$$U_i = (i-1)\Delta U \qquad i = 1, \ldots, k \qquad \Delta U = \frac{U_\infty}{k} \tag{10}$$

with the density of ten points per one electronvolt. The equations were solved for the values of E_0 from 0.25 kV cm^{-1} to 2.0 kV cm^{-1}; U_∞ was then set from 25 to 300 eV, and the number of mesh point was in the range 250–3000. A second order central finite difference formula was employed for the discretization approximating $\partial f_n(U_i)/\partial U$ by $(f_{n,i+1} - f_{n,i-1})/(2\Delta U)$, where $f_{n,i} = f_n(U_i)$. Thus the system of l partial differential equations was transformed into a system of kl ordinary differential equations. This system of ordinary differential equations for the values of f_n in the mesh points was solved by an explicit Runge–Kutta method of order 5(4) (DOPRI5 procedure [12]). This method for solution of time-dependent parabolic partial differential equations is a standard

method known as the method of lines (MOL). For a detailed introduction to the MOL see, e.g. [13]. The MOL is easy to implement in comparison with the method from [11] (for an overview of different implementations of MOL see [14]). The used MOL also does not exhibit any artificial oscillations at the same testing examples as the method from [11], which additionally uses an iterative treatment. The estimated error of the solution by our method was less than 0.1%. The described method was already successfully used for the study of electron relaxation in afterglow plasma [15]. However, the calculation of the full time-dependent solution of the equations given above for our conditions is not possible even with current computers. Assuming ionization to be a conservative process, fortunately the electron distribution function approaches the steady state distribution function very quickly after a change of E_0, as is shown below. So for a given E_0 the calculation was performed only until the steady state was reached. Because the changes in the rate coefficients during one period of the microwave power were less than 10%, for further calculation the rate coefficients were time averaged over one period. The values of time averaged rate coefficients as functions of E_0 were the results of these calculations. These rate coefficients were then used for the calculation of electron and excited nitrogen concentrations from the rate equations. A similar approach was used by Baeva *et al* [3]. The electron concentration can then be calculated from the equation:

$$\frac{\mathrm{d}n_\mathrm{e}(t)}{\mathrm{d}t} = n_\mathrm{e}(N\langle k_\mathrm{i}\rangle - \langle \nu_\mathrm{d}\rangle), \tag{11}$$

where $\langle k_\mathrm{i}\rangle$ is the time averaged ionization coefficient and $\langle \nu_\mathrm{d}\rangle = \langle D\rangle/\Lambda^2$, $\langle D\rangle$ is the time averaged diffusion coefficient and $\Lambda = R/\pi$ is the diffusion length. The losses of the electrons due to recombination can be neglected for the short times after the beginning of the microwave pulse. The electric field E_b corresponding to the breakdown can be obtained from the relation

$$N\langle k_\mathrm{i}\rangle(E_\mathrm{b}) = \langle \nu_\mathrm{d}\rangle(E_\mathrm{b}). \tag{12}$$

In the case of a pulsed discharge with a small repetition frequency (or a single pulse), breakdown occurs when the pulse duration t_p is sufficiently long so that the electron density equals the cut-off density before the end of the pulse [16]. The breakdown electric field is then obtained by solving the following equation:

$$N\langle k_\mathrm{i}\rangle(E_\mathrm{b}) - \langle \nu_\mathrm{d}\rangle(E_\mathrm{b}) = \frac{1}{t_\mathrm{p}}\ln(n_\mathrm{ec}/n_\mathrm{e0}), \tag{13}$$

where n_ec is the cut-off electron density ($1 \times 10^{18}\,\mathrm{m}^{-3}$ for frequency 9.4 GHz) and n_e0 is the initial electron density (in our case $\sim 10^8\,\mathrm{cm}^{-3}$). If the breakdown occurs at the time $t_\mathrm{b} \leqslant t_\mathrm{p}$, the breakdown electric field is higher as follows from (13) if t_p is substituted by t_b. The density of the microwave power absorbed in the plasma is given by the expression $\boldsymbol{j}\cdot\boldsymbol{E}$. Because the time resolved intensity of second positive system (SPS) of nitrogen was measured also, the concentration of nitrogen $C\,^3\Pi_\mathrm{u}$ state (in the following referred to as a C state) was calculated from the equation:

$$\frac{\mathrm{d}n_\mathrm{C}(t)}{\mathrm{d}t} = n_\mathrm{e}N\langle k_\mathrm{C}\rangle - \frac{n_\mathrm{C}}{\tau}, \tag{14}$$

where $\langle k_\mathrm{C}\rangle$ is the time averaged rate coefficient for the excitation to C state and τ is the time of life of this state. The intensity of SPS is then directly proportional to n_C.

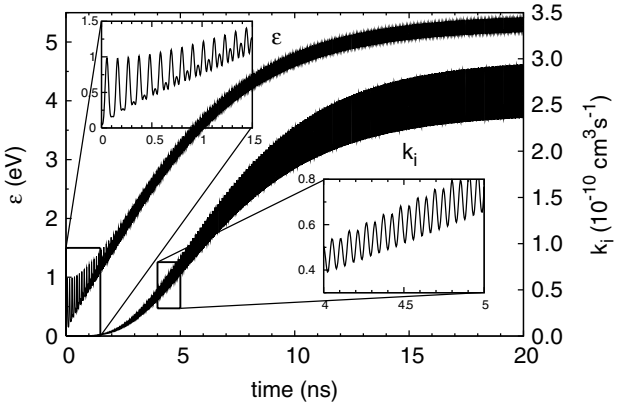

Figure 1. The time dependence of the mean electron energy and the ionization rate coefficient after the beginning of the microwave pulse. The nitrogen pressure was 100 Pa and the amplitude of electric field intensity E_0 was 1 kV cm^{-1}.

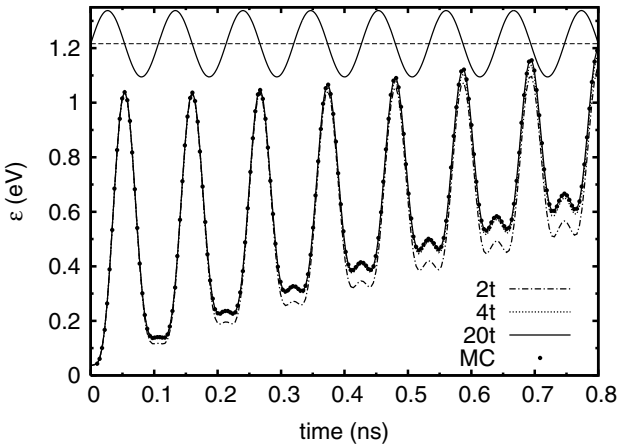

Figure 2. The time dependence of the mean electron energy after the beginning of the microwave pulse for different numbers of terms l in the distribution function expansion. The nitrogen pressure was 100 Pa and the amplitude of electric field intensity E_0 was 1 kV cm^{-1}. Dot-dashed line: $l = 1$, dotted line: $l = 3$, full line: $l = 19$. Full circles represent the results of Monte Carlo simulation. The time course of the electric field intensity is shown in the upper part of this figure.

4. Results and discussion

The time dependence of the mean electron energy and the ionization rate coefficient is shown in figure 1. The electric field $\boldsymbol{E} = E_0 \sin\omega t\boldsymbol{e}_z$ was switched on at $t = 0$, and the initial distribution function was chosen to be isotropic Maxwellian with a mean electron temperature of 300 K. As can be seen from figure 1 the mean electron energy reaches the steady state after ~20 ns. The time evolution of the electron distribution function together with a solution of electron particle balance was studied by Winkler and Wuttke in [17] for pulsed discharge in a mixture of Ne/Xe/HCl. They also came to the conclusion that the electron distribution function follows the changes of electric field intensity within tens of nanoseconds. The influence of the number of terms l in the expansion (2) on the accuracy of the calculated electron mean energy is demonstrated in figure 2. For a comparison, the values of the electron mean energy were obtained from a Monte Carlo simulation with 20 million electrons, and these values are

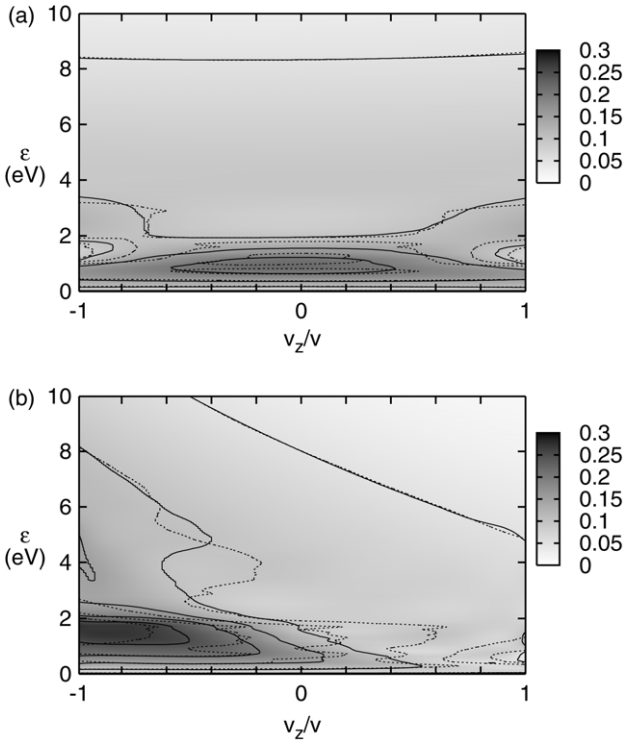

Figure 3. The electron distribution function in steady state for different electric field phase: full line: $l = 7$ and dashed line: $l = 1$. The nitrogen pressure was 100 Pa and the amplitude of electric field intensity E_0 was 1 kV cm^{-1}. (*a*) Maximum of electric field and (*b*) zero electric field.

represented by full circles in figure 2. It can be seen from this figure that the use of the usual two-term approximation leads to large errors in the calculated electron mean energy, and these errors increase with time. However, the values of the electron mean energy obtained from the solution of Boltzmann equation with $l = 19$ agree very well with the Monte Carlo values. Also in [18] it was found that the multi-term approach is necessary for the solution of the time-dependent electron Boltzmann equation in rf fields. The higher E_0 is, the higher the l to be chosen. Therefore the large value $l = 150$ was chosen for all the calculations.

The electron distribution function in steady state for different electric field phase is shown in figure 3. In this figure the function $U^{1/2}F(v(U), v_z/v, t)$ is plotted because it has a meaning of distribution function for U and v_z/v. An eight-term approximation is sufficient for the steady state; however, a two-term approximation is not sufficient and it exhibits artificial oscillations, see figure 3.

For the steady states at different values of E_0 the macroscopic parameters (mean energy, rate coefficients, etc) were calculated, and their values were averaged during one period of microwave power. The averaged values of ionization rate coefficient together with the averaged values of mean energy are plotted in figure 4; there are also the results obtained by the conventional EFA [19]. It can be seen that this approximation exhibits large discrepancies (30% for ionization rate coefficient) primarily for higher values of E_0 in comparison with the 'accurate' multi-term approximation. The averaged values of collision frequency and diffusion

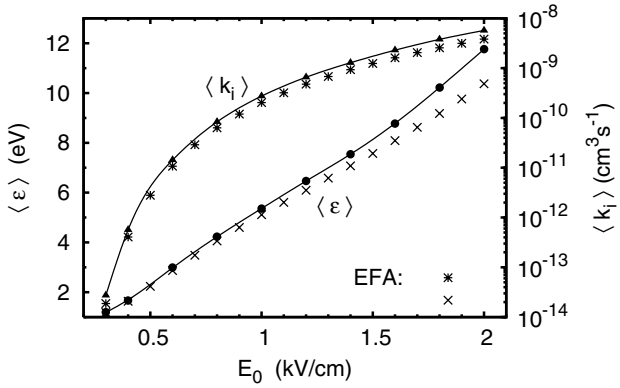

Figure 4. The dependence of the steady state time averaged mean electron energy and ionization rate coefficient on the amplitude of electric field intensity in microwave discharge at nitrogen pressure 100 Pa. Mean electron energy: circles; ionization rate coefficient: triangles. Crosses and stars represent the results obtained by (two-term) EFA.

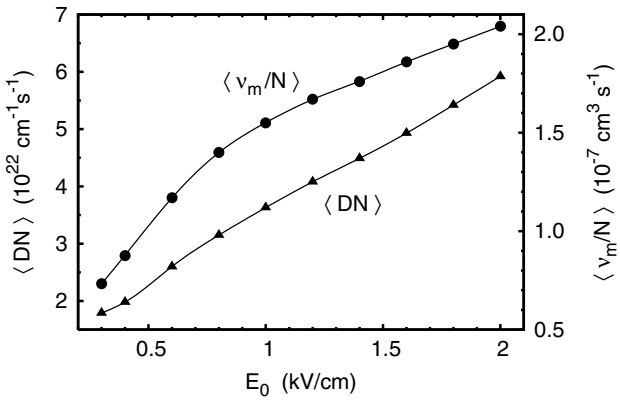

Figure 5. The dependence of the steady state time averaged collision frequency and diffusion coefficient on the amplitude of electric field intensity in microwave discharge at nitrogen pressure 100 Pa. Collision frequency: circles; diffusion coefficient: triangles.

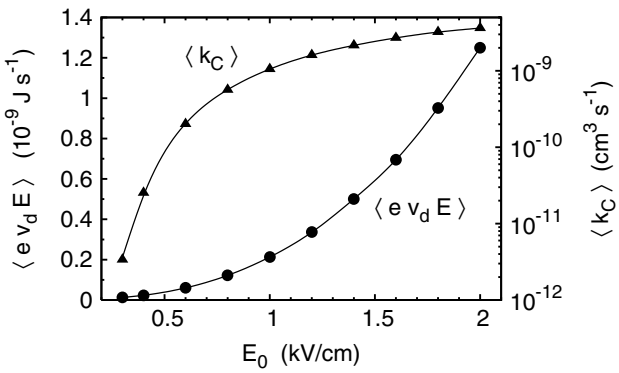

Figure 6. The dependence of the steady state time averaged rate coefficient for the excitation to C state and $\langle ev_{\mathrm{d}}E\rangle$ on the amplitude of electric field intensity in microwave discharge at nitrogen pressure 100 Pa. Rate coefficient: triangles; $\langle ev_{\mathrm{d}}E\rangle$: circles.

coefficient are shown in figure 5 and the averaged values of excitation rate coefficient for C state and $ev_{\mathrm{d}}E$ are shown in figure 6; all these quantities are shown as the functions of the amplitude of electric field intensity E_0. For the calculation of

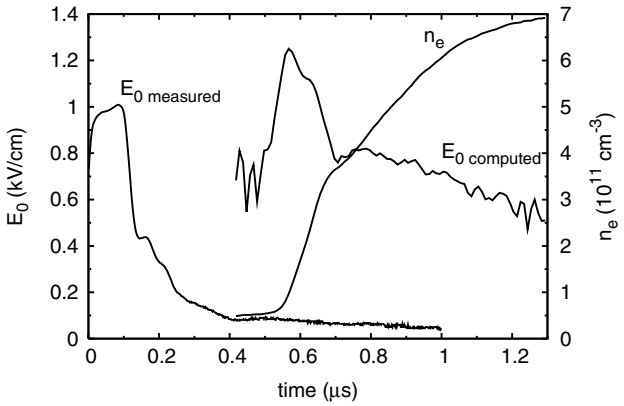

Figure 7. The comparison of measured and calculated electric field intensity. n_e is the measured electron concentration from [2].

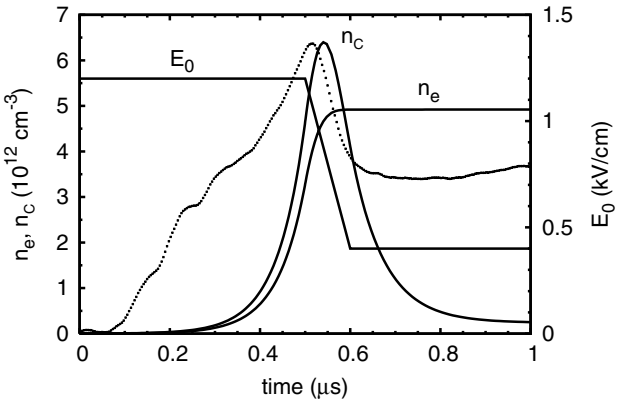

Figure 8. The time dependence of the intensity of SPS of nitrogen, (it is directly proportional to n_C) and electron concentration. The time dependence of E_0 was chosen as initial data for the calculation. The time dependence of intensity of nitrogen SPS measured in experiment [2] is plotted by crosses. The maximum value of measured intensity was set to the maximum value of n_C.

macroscopic quantities (mean energy, absorbed power, etc) at the real conditions of the experiment, it is necessary to know the corresponding value of E_0. Unfortunately, this value is not usually known. In our previous experiment [2] the time dependence of electron concentration was measured. So we decided to calculate the amplitude of electric field intensity just from the time dependence of electron concentration using equation (11). The measured time dependence of the electron concentration was differentiated, and the electric field intensity was then determined from equation (11) using calculated values of $\langle k_i \rangle$ and $\langle \nu_d \rangle$. The results are shown in figure 7. The breakdown field calculated for breakdown time $t_b = 0.2\,\mu s$ from (13) is $1.67\,\mathrm{kV\,cm^{-1}}$. The time dependence of the calculated electric field from figure 7 has the maximum value of $1.25\,\mathrm{kV\,cm^{-1}}$, and it is also shifted to longer times in comparison with measured electric field. In the experiment the discharge was ignited in the centre of the vessel, where the highest electric field intensity was, and then the plasma expanded. Finally the plasma ball was created. The microwave power was absorbed in the plasma, alternatively it could be reflected. The electric field was measured by an antenna behind the plasma ball, where the microwaves were dumped by the plasma. Also the measured electron concentration represents the average value of electron concentration across the plasma layer between the measuring antennae. Therefore the decrease of calculated electric field has to be shifted to longer time in comparison with the time development of the measured electric field. The plasma in the experiment had a radius of approximately 7.5 cm and the average electron concentration during the pulse was $10^{12}\,\mathrm{cm^{-3}}$. Then the power absorbed in the plasma at the electric field intensity $0.8\,\mathrm{kV\,cm^{-1}}$ calculated using the values from figure 6 is about 100 kW.

The intensity of SPS of nitrogen was also calculated from the electric field intensity and electron concentration data in figure 7. However, in this case the peak (the so-called overshoot [20]) in the intensity of SPS was not observed. So we tried to calculate the intensity of SPS for an artificially chosen time dependence of electric field intensity. The initial value of E_0 of this time dependence was roughly chosen from the experiment, and the decrease of the electric field was shifted to longer times so that the calculated values approximately correspond to the measured data. However, we did not try to fit them completely. The results of this calculation are shown in figure 8. The C state and the electron concentrations were calculated using equations (11) and (14); the initial electron concentration was chosen as $10^9\,\mathrm{cm^{-3}}$. The maximum of the calculated intensity of SPS is shifted by 25 ns to longer times in comparison with the maximum of measured intensity. This fact and the more gradual increase of measured intensity indicate that the initial electric field intensity was higher than was chosen.

5. Conclusion

The pulsed microwave discharge burning in nitrogen under the conditions described in [2] was studied theoretically. The electron distribution function was obtained by the numerical solution of time-dependent Boltzmann equation in multi-term approximation. It was shown that the macroscopic quantities (mean energy, collision frequencies, etc) do not change significantly during one period of microwave power, and therefore their time averaged values can be used for further calculation. It was also shown that the electron distribution function relaxes very quickly to its steady state, at which the electron distribution function does not depend on the previous history and depends only on the electric field amplitude E_0 for a given nitrogen pressure. So the time averaged rate coefficients were calculated as the functions of E_0 only. Then the continuity equation for electrons could be solved, and for the electron concentration obtained from the experiment the corresponding electric field amplitude was determined. The breakdown electric field amplitude was also calculated. The obtained electric field amplitudes are in qualitative agreement with experimental values. Finally, the calculated intensity of nitrogen SPS shows an analogous time course to the measured intensity.

Acknowledgment

We are grateful to the Czech Science Foundation for financial support under contracts No 202/03/0827 and 202/03/H162.

References

[1] Baeva M, Luo X, Pfelzer B, Schäfer J H, Uhlenbusch J and Zhang Z 1999 *Plasma Sources Sci. Technol.* **8** 142

[2] Meško M, Bonaventura Z, Vašina P, Kudrle V, Tálský A, Trunec D, Frgala Z and Janča J *Plasma Sources Sci. Technol.* in press

[3] Baeva M, Luo X, Pfelzer B and Uhlenbusch J 1999 *Plasma Sources Sci. Technol.* **8** 404

[4] Meško M, Bonaventura Z, Vašina P, Tálský A, Frgala Z, Kudrle V and Janča J 2004 *Plasma Sources Sci. Technol.* **13** 562

[5] Capitelli M personal communication see also ftp://ftp.muni.cz/pub/muni.cz/physics/data/N_2/

[6] Braglia G L, Wilhelm J and Winkler R 1985 *Lett. Nuovo Cimento* **44** 257

[7] Loffhagen D and Winkler R 1996 *Plasma Sources Sci. Technol.* **5** 710

[8] Petrovic Z L, Raspopovic Z M, Dujko S and Makabe T 2002 *Appl. Surf. Sci.* **192** 1

[9] White R D, Ness K F and Robson R E 2002 *Appl. Surf. Sci.* **192** 26

[10] Winkler R, Loffhagen D and Sigeneger F 2002 *Appl. Surf. Sci.* **192** 50

[11] Loffhagen D and Winkler R 1996 *J. Phys. D: Appl. Phys.* **29** 618

[12] Hairer R, Norsett S P and Wanner G 1993 *Solving Ordinary Differential Equations I. Nonstiff Problems* (Berlin: Springer)

[13] Schiesser W E 1991 *The Numerical Method of Lines* (San Diego, CA: Academic)

[14] Wang R, Keast P and Muir P 2004 *ACM Trans. Math. Softw.* **30** 454

[15] Trunec D, Spanel P and Smith D 2003 *Chem. Phys. Lett.* **372** 728

[16] MacDonald A D 1966 *Microwave Breakdown in Gases* (New York: Wiley)

[17] Winkler R and Wuttke M W 1992 *Appl. Phys.* B **54** 1

[18] Loffhagen D, Braglia G L and Winkler R 1998 *Contrib. Plasma Phys.* **38** 527

[19] Kortshagen U 1995 *Plasma Sources Sci. Technol.* **4** 172

[20] De Benedictis S, Dilecce G and Simek M 1999 *J. Chem. Phys.* **110** 2947